Optimal traffic control via time-gap regulation

Claudio Roncoli

Aalto University, Espoo 02150, Finland
(e-mail: claudio.roncoli@aalto.fi)

Abstract

We consider the problem of integrated traffic control in the presence of connected and automated vehicles, in particular by investigating the potential of time-gap regulation. Based on car-following models for semi-automated vehicles, we derive a macroscopic first-order traffic flow model that is employed to formulate a linearly constrained optimal control problem. Simulation results demonstrate improvements in term of traffic efficiency that may be achieved implementing the proposed strategy, also in comparison with conventional traffic control strategies.

1 Introduction

Recent developments in vehicle connectivity and automation have speed up the appearance of Connected and Automated Vehicles (CAVs) in our roads. In spite of a vast body of research that addressed technological developments for CAVs (Bishop, 2005), only a limited amount of studies investigated the impact of CAVs on traffic flow (Diakaki et al., 2015). Most of such works aim at capturing the impact of CAVs on traffic flow under different settings and penetration rates, using either microscopic simulation or macroscopic approaches (Bose and Ioannou, 2003; van Arem et al., 2006; Ntousakis et al., 2015; Mahmassani, 2016). Despite numerical results are sometimes in disagreement, general conclusions that may be drawn from those studies are that: (a) CAVs have the potential to improve or deteriorate, depending on their settings, the traffic conditions compared with the case of conventional manually driven vehicles; and (b) the level of the influence is closely related to the CAV penetration rate.

A recent stream of research investigated potential of traffic control strategies applied to CAVs, by employing conventional and new actuators (Schakel and van Arem, 2014; Papageorgiou et al., 2015; Roncoli et al., 2015; Khondaker and Kattan, 2015; Roncoli et al., 2016, 2017; Piacentini et al., 2018). In particular, CAVs provide the opportunity of having access to control actions that are otherwise not available with conventionally driven cars (e.g., individual vehicle speed, gap, or lane-change advice).

We focus here on CAVs with speed and time-gap regulation capabilities, via systems such as Adaptive Cruise Control (ACC) and Cooperative ACC (CACC). ACC systems are already widely appearing on the market; however, they are mainly designed to increase driving comfort and safety, which may imply conservative values for the ACC system settings (i.e., large time gaps and low accelerations). As an example, the suggested time-gap for current existing vehicles is in the order of 2 $\div$ 2.2 s, which is considerably higher compared to conventional manual driving vehicle traffic (van Arem et al., 2006; Milanés and Shladover, 2014). In case such settings are employed by a large number of drivers, this will eventually lead to the degradation of the static and dynamic road capacity, with more frequent and intense traffic congestion than nowadays. On the other hand, such systems have also the capability of achieving time-gaps that are lower than the ones appearing in conventional manual driving, e.g., up to 0.8 s in ACC systems and 0.6 s (and below) for CACC systems. Having the possibility to affect in real-time such settings, for example by delivering recommended time-gaps to an on-board console or by directly applying them to ACC/CACC systems within CAVs, would allow to improve the flow efficiency when critical traffic states are imminent or present. Few studies have advanced in this direction, by proposing the adaptation of ACC settings based on prevailing conditions, determined at vehicle or infrastructure level (Kesting et al., 2008; Schakel and van Arem, 2014; Goñi-Ros et al., 2016). Finally, Spiliopoulou et al. (2018) proposed an ACC-based control strategy to adapt in real time the driving behaviour of ACC-equipped vehicles to the prevailing traffic conditions so that motorway traffic flow efficiency is improved. Despite the proposed methods are shown to be efficient in improving or resolving local congestion, there are no research works dealing with such problem from an integrated traffic control perspective, accounting for the possibility of a combination of traffic control tasks (e.g., flow control via speed limits), as well as allowing for considering various infrastructure characteristics (e.g., various on- and off-ramps).

This paper presents a modelling framework and an optimal control problem formulation for integrated road traffic control, assuming the presence of CAVs with vehicle-to-infrastructure (V2I) communication and speed-gap regulation capabilities. The control strategy is designed so that it enables the regulation of CAV desired gaps, as well as variable speed limit control and ramp metering (if available or necessary). The approach is based on optimisation techniques applied to a dynamic traffic flow model opportunely defined to include only linear constraints, which allows for consideration of large-scale traffic networks with moderate computational effort.

2 Problem definition

The basic architecture considers a central Decision Maker (DM) that computes the solution of an optimisation problem, disaggregates the results and assigns specific vehicle control tasks that are sent for execution by the corresponding equipped vehicles. It is assumed that the DM has the complete knowledge of the traffic state when necessary; this may be achieved directly if all vehicles are CAVs and in communication with the infrastructure (V2I), or via an appropriate state estimation algorithm (Herrera and Bayen, 2010; Bekiaris-Liberis et al., 2016; Seo et al., 2017).

We proceed now by analysing the car-following behaviour of CAVs, in order to derive a traffic flow model, which will be later employed for optimisation.

2.1 Car following control law

This section details the relationship between semi-automated car-following models and macroscopic traffic flow models, starting from a realistic ACC-type car following control law and deriving a flow-density relationship. Let us start by considering car following laws adopted for semi-automated traffic, currently already employed within ACC vehicles (Milanés and Shladover, 2014). A controller for ACC is characterised by two control modes: a speed regulation mode, applied when the distance from the preceding vehicle is smaller than a given threshold (determined as function of the on-board sensors' detection range), and a gap regulation mode, applied otherwise.

The system dynamics for vehicles $c = 0, \dots,$ operating an ACC system can be described by

$$\dot{s_c} = v_c - v_{c-1} \tag{1}$$

$$\dot{v_c} = a_c, \tag{2}$$

where s is the bumper-to-bumper distance between vehicle c and the preceding vehicle $(c-1)$, while v_c and a_c denote, respectively, the speed and acceleration of vehicle c. Acceleration is computed as follows

$$a_c = \begin{cases} k_1 \left(v_c^{\mathrm{d}} - v_c \right), & \text{if } c \text{ is in speed regulation mode} \quad \text{(3a)} \\ k_2 \left(s_c - h_c^{\mathrm{d}} \, v_c \right) + k_3 \left(v_{c-1} - v_c \right), & \text{otherwise,} \quad \text{(3b)} \end{cases}$$

where v_c^{d} and h_c^{d} are the desired speed and time headway set by vehicle c, respectively, and k_1, k_2, k_3 are control gains appropriately specified. In order to obtain a macroscopic flow-density relation, we first derive the steady-state equilibrium of the car-following models above; we then proceed by deriving flow-density relations assuming stationary traffic conditions around each vehicle.

2.2 Speed regulation mode

In speed regulation mode, the steady-state equilibrium is obtained by employing (1), (2) and (3a), resulting in

$$v_c = v_{c-1} = v_c^{\mathrm{d}}. \tag{4}$$

Equation (4) implies that, assuming steady-state conditions, all vehicles travels at their desired speed v_c^{d}. If we further assume that the desired speed of all vehicles is the maximum speed on the road $v^{\max}$, dictated, e.g., by its speed limit, the resulting flow in speed regulation mode is

$$q = v^{\max} \rho \tag{5}$$

where q and ρ denote traffic flow and density respectively.

2.3 Gap regulation mode

In gap regulation mode, the steady-state equilibrium is obtained by employing (1), (2), (3b), resulting in

$$v_c = v_{c-1} = \frac{1}{h_c^{\mathrm{d}}} s_c. \tag{6}$$

Since (6) shows that the speed in gap regulation mode is constant for all vehicles, let us denote the resulting speed $\bar{v} = v_c$. We then introduce the average desired time headway for ACC-equipped vehicles $\bar{h}^{\mathrm{d}}$ and, because of the constant speed, we can write

$$\bar{v} = \frac{1}{\bar{h}^{\mathrm{d}}}\bar{s}, \tag{7}$$

where $\bar{s}$ is the average bumper-to-bumper distance. In order to obtain a micro–macro relation between the distance gap $\bar{s}$ and the density ρ, we directly apply the definition of the density as number of vehicles per road length. Assuming a constant (or average) vehicle length L, we have

$$\bar{s} = \frac{1}{\rho} - L, \tag{8}$$

which, replacing (8) into (7), allows to obtain the resulting flow in gap regulation mode

$$q = -LH\rho + H, \tag{9}$$

where $H = \frac{1}{\bar{h}^{\mathrm{d}}}$.

Note that, in case of CACC systems, despite a different controller (3b), the resulting steady state equilibrium (and, consequently, also the flow-density relation) is the same as shown here.

2.4 Macroscopic flow-density relation for CAV traffic

The car-following relations (5) and (9) may be used to derive a macroscopic flow-density relation for semi-automated traffic, which is shown in Figure 1. The resulting shape is the one of a triangular fundamental diagram, which is well known and employed in several traffic studies (e.g., CTM, Daganzo, 1994). In conventional traffic, which involve the consideration of only manual driven vehicles, the fundamental diagram is a result of specific road configuration and drivers' behaviour (Treiber and Kesting, 2013). Differently, in the presence of CAVs, we observe that the choice of desired time headway affects significantly the traffic characteristics, above all the maximum achievable flow, commonly known as capacity.

Note that we do not refer deliberately to free flow and congested regime since being on a different point of the fundamental diagram is result of a specific set of controller parameters and not necessary related to the appearance of congestion.

For optimal control design, we assume controllable the longitudinal flows, via corresponding adjustments of CAV speeds and time-gaps, as mentioned earlier. Hence, the lines of the piecewise-linear FD of Figure 1 are simply used as upper bounds for the controllable longitudinal flows, in a similar fashion as what employed by Ziliaskopoulos (2000); Gomes and Horowitz (2006); Roncoli et al. (2015).

3 Problem formulation

We consider a road network that is subdivided into $n = 0, \dots, N$ segments of length Δ_i and we formulate our model in discrete time, considering time-step T, by introducing $k = 0, 1, \dots, K$, where the time is $t = kT$. Each segment is characterised by traffic density $\rho_n(k)$, i.e., the number of vehicles in segment n at time k divided by the

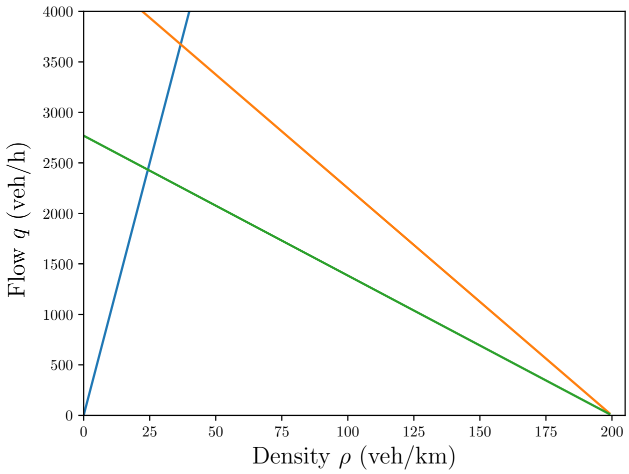

Figure 1: The resulting fundamental diagram. The speed regulation part is obtained for $v^{\max} = 100$ km/h; while the gap regulation part is obtained for $\bar{h}^{\mathrm{d}} = 1.3$ s (green line) and $\bar{h}^{\mathrm{d}} = 0.8$ s (orange line).

segment length Δ_n; and the total outflow $q_n(k)$, i.e., the number of vehicles leaving segment n during time interval $(k, k+1]$. We denote the set of segments immediately downstream of segment n as Φ_n and the set of segments immediately upstream of n as Γ_n.

Density dynamically evolves according to the following conservation law equation

$$\rho_n(k+1) = \rho_n(k) + \frac{T}{\Delta_n}\left[\sum_{p\in\Gamma_n} q_{p,n}(k) - \sum_{m\in\Phi_n} q_{n,m}(k) + d_n(k)\right], \tag{10}$$

where $d_n(k)$ is the flow entering the traffic network at segment n.

Depending on the network topology, we have different formulations for computing flows at each segment, as follows.

3.1 Ordinary segment

We define ordinary segments as those that have only have a segment upstream and a segment downstream: $|\Gamma_n| = |\Phi_n| = 1$. Density evolves according to (10), while $d_n(k) = 0$. For an ordinary segment n, the following constraints are introduced

$$q_n \leq v_n^{\max}\rho_n \tag{11}$$

$$q_n \leq \frac{v_n^{\max}H_n}{v_n^{\max} + LH_n} \tag{12}$$

$$q_m \leq -LH_n\rho_n + H_n \tag{13}$$

$$q_m \leq \frac{v_n^{\max}H_n}{v_n^{\max} + LH_n}, \tag{14}$$

where $m \in \Gamma_n$.

3.2 Source segment

We define source segments as those that have only a segment downstream: $|\Gamma_n| = 0$, $|\Phi_n| = 1$, while flow can enter from outside the traffic network. Density evolves according to (10). In addition, we consider the possibility of controlling the external inflow (e.g., via ramp metering) and we introduce dynamics of queue length $w_n(k)$, defined as

$$w_n(k+1) = w_n(k) + T\left[D_n(k) - d_n(k)\right], \tag{15}$$

where $D_n(k)$ is the external inflow expected to enter the traffic network. Queues are upper bounded by corresponding maximum queue length $w_n^{\max}$. Constraints defined for a source segment n are therefore (11), (12), and

$$d_n \leq -LH_n\rho_n + H_n \tag{16}$$

$$d_n \leq \frac{v_n^{\max} H_n}{v_n^{\max} + LH_n} \tag{17}$$

$$w_n \leq w_n^{\max}. \tag{18}$$

3.3 Sink segment

We define sink segments as those that have only a segment upstream: $|\Gamma_n| = 1$, $|\Phi_n| = 0$, while the corresponding outflow is expected to exit the network. Density evolves according to (10), where $d_n(k) = 0$, and related constraints are (13) and (14).

3.4 Merging segment

We define merging segments as those that have one segment downstream and more than a segment upstream: $|\Gamma_n| > 1$, $|\Phi_n| = 1$. Density evolves according to (10), while $d_n(k) = 0$. In order to account for the capacity drop phenomenon, i.e. the reduction of discharge flow once queues start forming at a bottleneck location (Cassidy and Bertini, 1999), we consider a linearly decreasing function that affects the merging segment in case at least one of the upstream segments is congested, in a similar way as proposed by Kontorinaki et al. (2017). Constraints defined for a merging segment n are therefore (11), (12), and

$$\sum_{m\in\Gamma_n} q_m \leq -LH_n\rho_n + H_n \tag{19}$$

$$\sum_{m\in\Gamma_n} q_m \leq \frac{v_n^{\max} H_n}{v_n^{\max} + LH_n} \tag{20}$$

$$\begin{aligned}\sum_{m\in\Gamma_n} q_m \leq & -\frac{(1-\beta)\, v_n^{\max} LH_n \left(v_\ell^{\max} + LH_\ell\right)}{v_\ell^{\max}\left(v_n^{\max} + LH_n\right)}\rho_n\ell(k) \\ & + \frac{\beta\, v_n^{\max} H_n}{v_n^{\max} + LH_n} + \frac{(1-\beta)\, v_n^{\max} H_n \left(v_\ell^{\max} + LH_\ell\right)}{v_\ell^{\max}\left(v_n^{\max} + LH_n\right)}, \qquad \forall \ell \in \Gamma_n,\end{aligned} \tag{21}$$

where $\beta \leq 1$ is a capacity drop-related parameter.

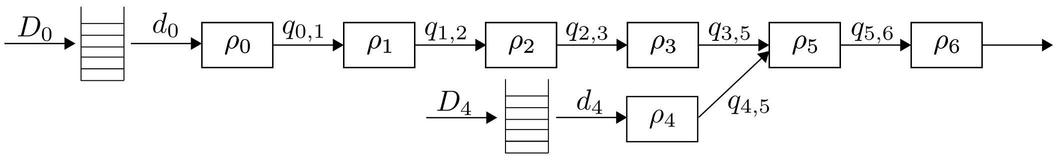

Figure 2: The network used in the simulation scenarios.

3.5 Cost function

The resulting optimisation problem reads as follows

$$\min \sum_{k=1}^{K} \sum_{n=0}^{N} \left[T \left[\Delta_n \rho_n(k) + w_n(k) \right] + \frac{1}{2} \alpha \left[q_n(k) - q_n(k-1) \right]^2 \right] \tag{22}$$

subject to linear equalities (10), (15) and linear inequalities (11)–(14), (16)–(21).

The cost function (22) is composed of two terms:

- A linear term corresponding to Total Time Spent (TTS), which accounts both for the time travelled and the time spent queuing at on-ramps; this is the most important term that is used to evaluate the goodness of the solution in terms of traffic flow efficiency.
- A quadratic penalty term, weighted by parameter α, aiming at penalising the variation of control variables (i.e., flow) from a time step to the next one, which is introduced in order to reduce, or even suppress, space–time fluctuations of the control variables that have a minor contribution to the resulting traffic flow efficiency.

The formulated discrete-time optimal control problem is in the form of a (linearly constrained) quadratic optimization problem, which can be solved very efficiently using available numerical solution codes, even for large-scale infrastructures.

4 Results

We introduce a simple road network, composed of $N = 7$ segments, which are connected as illustrated in Figure 2. All segments in the network are characterised by the same length $\Delta_n = 0.5$ km and the same maximum speed $v_n^{\max} = 90$ km/h; moreover, we assume that, without intervention of specific control, vehicles travel with a time-gap $h_n^{\mathrm{d}} = 1.3$ s, which is a reasonable value observed for conventional traffic (Treiber and Kesting, 2013). Average vehicle length is set as $L = 4$ m, while parameter for capacity drop is set as $\beta = 0.9$. We feed the network with a constant demand D_0 and a trapezoidal-like demand D_4, as shown in Figure 3(a). Density is initialised as $\rho_n(0) = 10$ veh/km. In this network, we can observe a potential bottleneck at merging segment 5, which would be activated in case the entering demand exceeds its capacity.

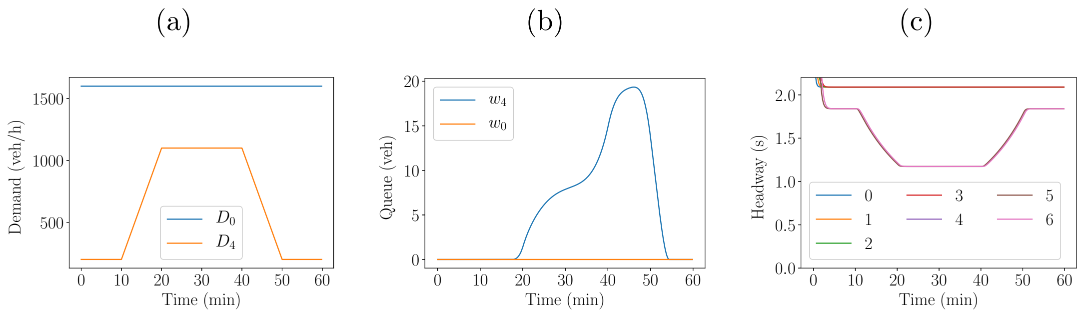

Figure 3: (a) The traffic demand used in the simulation scenarios. (b) Queues created in the conventional control scenario. (c) Time-gaps resulting in the time-gap regulation scenario.

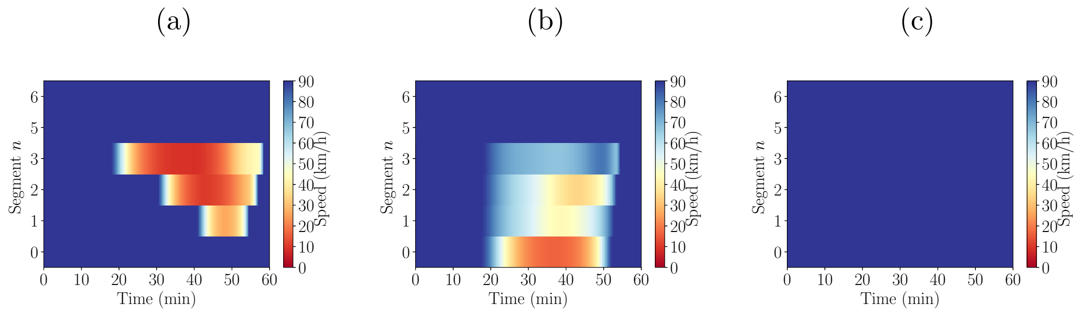

Figure 4: Simulation results for (a) no-control case; (b) control via ramp metering and variable speed limits, without gap regulation; via gap regulation.

4.1 No-control scenario

The first scenario is the so-called no-control case, which is used as a basic case for performance evaluation of the proposed control strategy. In this scenario, we assume that vehicles' behaviour is not influenced by external control decision, i.e., vehicles move at the maximum speed $v_n^{\max}$, unless a developing congestion constraints their movement. This is implemented by a CTM-like model with capacity drop, which basically implements the model described in Section 3. The formulation is not included here due to space limitations. Note that, in this scenario, no optimisation is performed.

The resulting speed profiles in all segments of the mainstream are shown in Figure 4 (a), where we can observe that a congestion develops upstream of the merging segment (as expected in a first-order model, see Kontorinaki et al. 2017). The reason for congestion is that, around $t = 20$ min, i.e., when the demand at D_4 reaches its maximum, the overall demand at segment 5, which is a merging segment accepting flow from both segments 3 and 4, is higher than its corresponding capacity, causing the activation of the bottleneck. Because of the high density in segments 3 and 4, capacity drop is triggered, causing a reduction of the flow allowed in segment 5. The congestion spills back until segment 1 and lasts until the demand at D_4 decreases. The resulting TTS for the no-control scenario is TTS $=$ 107.14 veh$\cdot$h.

4.2 Conventional control scenario

This scenario investigates the traffic condition mitigation that are achievable via employing "conventional" actuators, i.e., ramp metering and mainstream flow control, where the latter may be implemented, e.g., via variable speed limits. We implement the scenario by solving the optimisation problem (22), (10)–(21), using the following parameters: $w_0^{\max} = 0$, $w_4^{\max} = 20$ veh, $\alpha = 10^{-8}$.

The resulting speed profiles in all segments of the mainstream are shown in Figure 4 (b), where we can observe that a controlled congestion (i.e., not due to bottleneck activation, but to decisions of the optimisation problem) develops far upstream of the merging segment, namely in segments 0, 1, and 2. In addition, ramp metering actions take place at the entrance of segment 4, causing a queue to develop (see Figure 3 (b)). It is interesting noting that the controlled congestion has a higher internal speed than the one observed in the no-control case. The resulting TTS for this scenario is TTS $=$ 94.19 veh·h, which corresponds to an improvement of 12.1% with respect to the no-control case.

4.3 Time-gap regulation scenario

The last scenario investigates the case when, besides conventional traffic control measures, we assume that the DM is capable of influencing the time gap implemented by semi-automated vehicles. We implement this scenario by solving the optimisation problem (22), (10)–(21), allowing the optimiser to assign a lower time-gap to traffic; in this scenario, we employ $h_n^{\mathrm{d}} = 0.8$ s. All the remaining parameters are maintained as in the previous scenario.

The resulting speed profiles in all segments of the mainstream are shown in Figure 4 (c), where we can observe that no congestion is appearing in the network; in addition, no queue at ramp is created. As can be observed by inspecting Figure 3 (c), these results are achieved by a decrease of the time-gap of vehicles travelling in segment 5 and 6 during the period characterised by high demand. A reduced time-gap in such segments produce a higher capacity, which allows to accommodate all the demand, without triggering any congestion. The minimum time-gap in segment 5 and 6 is, for this scenario, in the order of 1 s, which would be the desired time gap ordered/recommended to CAVs travelling on these segments. In case the penetration rate of CAVs is lower than 100%, the same outcome can be achieved, e.g., by assigning 40% of vehicles (CAVs) to employ a time-gap of 0.8 s (assuming other vehicles drive at an average time-gap of 1.3 s). The resulting TTS is TTS $=$ 64.81 veh·h, which corresponds to an improvement of 39.5% with respect to the no-control case.

5 Conclusions

The paper presents an optimisation-based approach for traffic control in presence of CAVs, exploiting the possibility of regulating desired time-gaps and communication capabilities. The optimal control has generated important and useful results, showing that the use of such strategy could enable strong benefits in term of traffic efficiency. Ongoing work include the validation of the developed model and optimal control problem using microscopic simulation.

References

Bekiaris-Liberis, N., C. Roncoli, and M. Papageorgiou (2016). Highway traffic state estimation with mixed connected and conventional vehicles. *IEEE Transactions on Intelligent Transportation Systems 17*, 3484–3497.

Bishop, R. (2005). *Intelligent vehicle technology and trends.* Artech House Publishers.

Bose, a. and P. Ioannou (2003). Analysis of traffic flow with mixed manual and semi-automated vehicles. *IEEE Transactions on Intelligent Transportation Systems 4*(4), 173–188.

Cassidy, M. J. and R. L. Bertini (1999). Some traffic features at freeway bottlenecks. *Transportation Research Part B: Methodological 33*(1), 25–42.

Daganzo, C. F. (1994). The cell transmission model: A dynamic representation of highway traffic consistent with the hydrodynamic theory. *Transportation Research Part B: Methodological 28*(4), 269–287.

Diakaki, C., M. Papageorgiou, I. Papamichail, and I. K. Nikolos (2015). Overview and analysis of vehicle automation and communication systems from a motorway traffic management perspective. *Transportation Research Part A: Policy and Practice 75*, 147 – 165.

Gomes, G. and R. Horowitz (2006). Optimal freeway ramp metering using the asymmetric cell transmission model. *Transportation Research Part C: Emerging Technologies 14*(4), 244 – 262.

Goñi-Ros, B., V. L. Knoop, T. Takahashi, I. Sakata, B. van Arem, and S. P. Hoogendoorn (2016). Optimization of traffic flow at freeway sags by controlling the acceleration of vehicles equipped with in-car systems. *Transportation Research Part C: Emerging Technologies 71*, 1–18.

Herrera, J. C. and A. M. Bayen (2010). Incorporation of lagrangian measurements in freeway traffic state estimation. *Transportation Research Part B: Methodological 44*(4), 460 – 481.

Kesting, A., M. Treiber, M. Schönhof, and D. Helbing (2008). Adaptive cruise control design for active congestion avoidance. *Transportation Research Part C: Emerging Technologies 16*(6), 668–683.

Khondaker, B. and L. Kattan (2015). Variable speed limit: A microscopic analysis in a connected vehicle environment. *Transportation Research Part C: Emerging Technologies 58*, 146–159.

Kontorinaki, M., A. Spiliopoulou, C. Roncoli, and M. Papageorgiou (2017). First-order traffic flow models incorporating capacity drop: Overview and real-data validation. *Transportation Research Part B: Methodological 106*, 52–75.

Mahmassani, H. S. (2016). 50th anniversary invited article – Autonomous vehicles and connected vehicle systems: Flow and operations considerations. *Transportation Science 50*(4), 1140–1162.

Milanés, V. and S. E. Shladover (2014). Modeling cooperative and autonomous adaptive cruise control dynamic responses using experimental data. *Transportation Research Part C: Emerging Technologies 48*, 285–300.

Ntousakis, I. A., I. K. Nikolos, and M. Papageorgiou (2015). On microscopic modelling of adaptive cruise control systems. *Transportation Research Procedia 6*, 111 – 127.

Papageorgiou, M., C. Diakaki, I. Nikolos, I. Ntousakis, I. Papamichail, and C. Roncoli (2015). Freeway Traffic Management in Presence of Vehicle Automation and Communication Systems (VACS). pp. 205–214.

Piacentini, G., P. Goatin, and A. Ferrara (2018). Traffic control via moving bottleneck of coordinated vehicles. *IFAC-PapersOnLine 51*(9), 13–18.

Roncoli, C., N. Bekiaris-liberis, and M. Papageorgiou (2017). Lane-Changing Feedback Control for Efficient Lane Assignment at Motorway Bottlenecks. *Transportation Research Record: Journal of the Transportation Research Board 2625*, 20–31.

Roncoli, C., M. Papageorgiou, and I. Papamichail (2015). Traffic flow optimisation in presence of Vehicle Automation and Communication Systems - Part II: Optimal control for multi-lane motorways. *Transportation Research Part C 57*, 260 – 275.

Roncoli, C., I. Papamichail, and M. Papageorgiou (2016). Hierarchical model predictive control for multi-lane motorways in presence of Vehicle Automation and Communication Systems. *Transportation Research Part C: Emerging Technologies 62*, 117–132.

Schakel, W. J. and B. van Arem (2014). Improving traffic flow efficiency by in-car advice on lane, speed, and headway. *IEEE Transactions on Intelligent Transportation Systems 15*(4), 1597–1606.

Seo, T., A. M. Bayen, T. Kusakabe, and Y. Asakura (2017). Traffic state estimation on highway: A comprehensive survey. *Annual Reviews in Control 43*, 128–151.

Spiliopoulou, A., D. Manolis, F. Vandorou, and M. Papageorgiou (2018). Adaptive cruise control operation for improved motorway traffic flow. *Transportation Research Record: Journal of the Transportation Research Board 2672*(22), 24–35.

Treiber, M. and A. Kesting (2013). *Traffic Flow Dynamics.* Berlin, Heidelberg: Springer Berlin Heidelberg.

van Arem, B., C. J. G. van Driel, and R. Visser (2006). The impact of cooperative adaptive cruise control on traffic-flow characteristics. *IEEE Transactions on Intelligent Transportation Systems 7*(4), 429–436.

Ziliaskopoulos, A. K. (2000). A linear programming model for the single destination system optimum dynamic traffic assignment problem. *Transportation Science 34*(1), 37–49.